Carbohydrate Polymers 111 (2014) 598–605

Contents lists available at ScienceDirect

Carbohydrate Polymers

journal homepage: www.elsevier.com/locate/carbpol

FTIR characterization of protein–polysaccharide interactions in extruded blends

Pedro Guerrero [a], Joe P. Kerry [b], Koro de la Caba [a,*]

[a] BIOMAT Research Group, University of the Basque Country (UPV/EHU), Department of Chemical and Environmental Engineering, Polytechnic School, Donostia-San Sebastián, Spain
[b] Food Packaging Group, School of Food & Nutritional Sciences, University College Cork (UCC), Cork, Ireland

ARTICLE INFO

Article history:
Received 10 March 2014
Received in revised form 30 April 2014
Accepted 5 May 2014
Available online 14 May 2014

Keywords:
Proteins
Secondary structure
Polysaccharides
Interactions
FTIR

ABSTRACT

Soy protein-based blends were processed by double screw extrusion and the effects of different types and contents of polysaccharides were analyzed. Although extrusion has not been widely used for this type of blends, in this study it was observed that the increase in polysaccharide content in blends caused a decrease in specific mechanical energy (SME), facilitating extrusion process and showing the potential of this process, which is more cost effective at industrial scale. In order to explain this behavior, infrared spectroscopy analysis was carried out, mainly in the amide I and II regions. Moreover, curve fitting analysis showed the conformational changes produced in the blends due to the addition of polysaccharides, which affected protein denaturation. These changes also affected properties such as moisture content (MC) and total solubility matter (TSM). However, conformational changes did not show significant effects with respect to piece density (PD) or in the expansion ratio (ER) of the pellets. The quantitative analysis of the changes in the amide I and II regions provided novel information about the modifications produced in protein-based blends modified with polysaccharides. In this context, infrared spectroscopy provided a convenient and powerful means to monitor interactions between all ingredients used in the blend formulation, which is of great importance in order to explain changes in the functional properties of biodegradable materials used for industrial applications in food and pharmaceutical industries.

1. Introduction

Proteins and polysaccharides are biomacromolecules employed as functional ingredients. Mixtures of both types of biomacromolecules are often used in many technological applications, including food, pharmaceutical, and cosmetics industries (Andrade-Mahecha, Tapia-Blacido, & Menegalli, 2012; Archana et al., 2013; Guerrero, Etxabide, Leceta, Peñalba, & de la Caba, 2014; Salarbashi et al., 2013). Protein–polysaccharide conjugates are useful because such ingredient conjugates have improved functional properties, such as heat and pH stability, solubility, emulsification, and gelation properties, offering lower astringency and allergenicity compared to unmodified proteins (Doublier, Garnier, Renard, & Sanchez, 2000; Klein, Aserin, Ben Ishai, & Garti, 2010; Rodríguez & Pilosof, 2011). These properties, together with the increasing demands to control biochemical interactions at the tissue/material interface, have prompted scientists to investigate these systems. Nevertheless, the knowledge underpinning protein–polysaccharide interactions is still rather limited (Alves, Costa, & Coelhoso, 2010; Wang et al., 2014). In the specific context of protein-based blends, several factors such as protein concentration, pH, ionic strength, heating temperature, and plasticizers affect the formation of the blend. It has been suggested that the blend network is formed via hydrogen bonds and hydrophobic and electrostatic interactions. However, the structural basis of the blend-forming process is, at present, not fully understood. No attempt has been made to determine the relationship between the extent of formation of the blend network and the structure of the protein in the blend, and nothing is known about the molecular basis that leads to the formation of such blends.

The formation of blends from soy proteins and other globular proteins has been described as a heat denaturation process. Heating alters the three-dimensional structure of proteins, exposing functional peptide groups such as CO and NH and side chain polar and hydrophobic groups that are engaged in intramolecular hydrogen bonding and electrostatic interactions in the native state; therefore,

* Corresponding author at: Escuela Universitaria Politécnica, Departamento de Ingeniería Química y del Medio Ambiente, Plaza Europa 1, 20018 Donostia-San Sebastián, Spain. Tel.: +34 943 017188.
E-mail address: koro.delacaba@ehu.es (K. de la Caba).

http://dx.doi.org/10.1016/j.carbpol.2014.05.005
0144-8617/

these functional groups become available for further intermolecular interactions (Wang & Damodaran, 1991). The unfolded protein chains approach each other and become linked through intermolecular interactions, leading to the formation of a network that acts as the matrix for entrapping blend components such as plasticizing agents. Since the formation of a blend occurs upon application of denaturating conditions, it is quite possible that the denatured protein may undergo partial refolding, thus regaining some secondary structure during the blending process (Gilbert et al., 2005). It is conceivable that the extent of such refolding affects the number of functional groups available for intermolecular interactions and thus, the formation and stability of the blend network. Blends based on globular proteins are attractive materials because of their potential applications as edible or biodegradable coatings and wrappings. This type of matrix is also relevant for pharmaceutical and medical applications since it may be employed for the encapsulation and release in vivo of bioactive substances at specific sites and for the growth of cell cultures. A clear understanding of the structure and formation of blends is required to control their properties. Besides these applications, globular protein-based blends also arouse interest in the more fundamental aspects of chemical interactions involving their use since they may be helpful in providing insights into the interactions that govern protein self-assembly and protein conformation. In this context, many efforts have been devoted to the optimization of the techno-functional properties of soy proteins, which have received increasing attention since soy protein is a co-product of the soy oil industry and which can be valorized (Félix, Martín-Alfonso, Romero, & Guerrero, 2014; Leceta, Etxabide, Cabezudo, de la Caba, & Guerrero, 2014).

Regarding the processing of protein-based blends, the employment of extrusion is one of the most versatile and well-established processes used to produce macromolecular and polymeric materials (Galicia-García et al., 2011). Moreover, extrusion is relatively inexpensive (as the technology can be scaled to production volume and simplified for specific commercial usage) and amenable to industrial scale-up. Extrusion conditions, such as high barrel temperatures, high pressures and the use of low moisture during processing, bring about major conformational changes in the ingredient components in extrusion blends during processing. In addition, it is well-known that, among all of the different process variables that need to be considered during extrusion, the rate and amount that moisture is introduced into the extruder and the processing temperature employed at all critical points along the process have important effects on the quality of the final extruded products. It is generally accepted that proteins are denatured during the extrusion process, so these "reactive" unfolded protein chains can interact with each other, and with other added components, allowing the formation of a polymeric network. The role of covalent bonding on final product characteristics has been well documented since disulfide bonds were found to develop during this process (Fukushima & Van Buren, 1970a); however, physical interactions including hydrophobic effects and hydrogen bonding are clearly also involved (Fukushima & Van Buren, 1970b; Quinn, Monahan, O'Sullivan, & Langares, 2003), although the contribution of each type of interaction remains unclear. Most of the studies on blends have focused on a selected number of macroscopic characteristics attributable to the resulting films produced, such as stress and strain at break point, permeability to gases and vapors, and moisture absorption, among others. While the macroscopic properties of films made with globular proteins have been extensively investigated, only a limited amount of information exists with respect to their structure. Films made of soybean glycinin and wheat gliadin have been examined at a molecular level using Fourier transform infrared (FTIR) spectroscopy (Mangavel, Barbot, Popineau, & Gueguen, 2001; Subirade, Kelly, Gueguen, & Pezolet, 1998). These studies revealed the presence of intermolecular β-sheets following heating and dehydration steps which underline the importance of hydrogen bonding in the formation of the protein network. β-Sheets have been proposed to act as junction zones in the cohesion of film, and in the relationship between protein conformation and mechanical properties has been proposed (Mangavel et al., 2001). Such reports underline the role that the β-sheet motif may play in the structure and properties of globular protein films but more data are needed to evaluate the importance of this type of structure.

Since few data are available about the molecular events occurring during blend formation employing globular proteins, the aim of this work was to describe the protein conformational changes occurring during the extrusion process. The influence of heat treatment and the role played by different types and contents of polysaccharides on final structure were also considered. In order to elucidate the molecular basis pertaining to blend formation, conformational changes in the biomacromolecules employed in this study were investigated under extrusion conditions. In this investigation, infrared spectroscopy was employed to obtain detailed information on the molecular and conformational modifications occurring during the blending formation process since it has been well established that infrared spectroscopy is a powerful method for the investigation of secondary protein structures in complex systems, such as biological or food systems (Goormaghtigh, Cabiaux, & Ruysschaert, 1990; Guerrero, Garrido, Leceta, & de la Caba, 2013; Mangavel et al., 2001).

2. Materials and methods

2.1. Materials

Soy protein isolate (SPI), PROFAM 974, with 90% protein on a dry basis was supplied by Lactotecnia S.L. (Barcelona, Spain). The SPI employed in this study was comprised of 5% of moisture, 4% of fat and 5% of ash. It had an acid character and an isoelectric point of 4.6. The polysaccharides used in this study were obtained from Aldrich (Madrid, Spain), and included gum arabic (ARA) from acacia tree (G9752), dextran (DEX) from *Leuconostoc mesenteroides* (D5251), and carboxymethylcellulose (CMC) sodium salt (C4888). Glycerol (GLY) was used as the plasticizer in this study and this was obtained from Panreac (Barcelona, Spain).

2.2. Extruder and experimental configurations

A twin-screw extruder (MPF 19/25 APV Baker) was used in this study. The APV Baker MPF19 extruder was designed to generate the high pressures needed to extrude a wide range of products, in particular, edible/biodegradable blends. The MPF 19/25 possessed 19 mm diameter barrel, a length to barrel diameter ratio of 25:1, and a barrel comprising four controlled temperature zones, resulting in a die temperature of 70–100 °C.

2.3. Samples preparation

SPI, glycerol and polysaccharide contents required to obtain the desired blend composition were mixed. All components were mixed in a variable speed Stephan mixer, model UMC 5 (Stephan, UK), for 5 min at 1500 rpm. SPI was replaced (3, 6 and 9 wt%) by polysaccharide to obtain SPI–polysaccharide blends, and samples were designated as ARA3, ARA6 and ARA9 in the case of gum arabic, CMC3, CMC6 and CMC9 in the case of carboxymethylcellulose, and DEX3, DEX6 and DEX9 for dextran. Glycerol was selected at 30% (w/w), based on results obtained from previous work (Guerrero, Nur Hanani, Kerry, & de la Caba, 2011). The sample without polysaccharides was designated as the control. Mixtures were added into

the feed hopper and mixed with water in the barrel of the twin-screw extruder. All trials were carried out using a water speed of 2.94 g/min (0.15 kg/h). Water was pumped directly into the extruder barrel zone 1 using a peristaltic pump (504U MK, Watson Marlow Ltd.).

2.4. Specific mechanical energy (SME)

The specific mechanical energy was calculated using the expression (Hu, Hsieh, & Huff, 1993):

$$\text{SME (kJ/kg)} = \frac{\text{screw speed} \times \text{power (kW)} \times \text{torque (\%)}}{\text{max. screw speed} \times \text{throughput (kg/h)} \times 100}$$

The extruder was operated at a constant speed of 250 rpm. The feed rate of extruder was adjusted to 1 kg/h and had a 2 kW/h motor power in practice. Dies were scaled up by maintaining a constant throughput per unit of orifice area. The extruder was equipped with a single die of 3 mm diameter giving a throughput per unit area of 0.141 kg/h mm^2.

2.5. Piece density (PD)

Piece density is the density of each extrudate and was obtained by dividing the mass of extrudate piece (W_{piece}) by its volume (V_{piece}), which was computed from its dimensions (diameter, d; and length, l). The piece dimensions of ten, 2-cm long, pieces were measured by using a hand-held digimatic micrometer (QuantuMike Mitutoyo), and piece density was calculated as:

$$\text{PD} = \frac{W_{piece}}{V_{piece}} = \frac{4 \times W_{piece}}{\pi \times d^2 \times l}$$

2.6. Expansion ratio (ER)

The expansion ratio is the ratio of the extrudate cross-sectional area to the die orifice cross-sectional area, and was calculated as:

$$\text{ER} = \frac{d^2}{d_{die}^2}$$

where d_{die} is the die diameter and d is the extrudate diameter (average of 10 samples), which was measured by using a hand-held digimatic micrometer (QuantuMike Mitutoyo).

2.7. Moisture content (MC) and total soluble matter (TSM)

Three specimens of each sample were analyzed to determine moisture content and total soluble matter values according to a method previously used in several studies of proteins (Gontard & Guilbert, 1992; Kunte, Gennadios, Cuppett, Hanna, & Weller, 1997). Samples were weighed (m_w) and subsequently dried in an air-circulating oven at 105 °C for 24 h. After this time, samples were reweighed (m_0) to determine MC values. Samples were dried as an extrudate and MC values were calculated as:

$$\text{MC (\%)} = \frac{m_w - m_0}{m_w} \times 100$$

Afterwards, samples were immersed in 30 mL of distilled water in the presence of sodium azide (0.02%) in order to prevent microbial growth. The beakers were stored in an environmental chamber at 25 °C for 24 h with occasional gentle stirring. After this time, specimens were dried in an air-circulating oven at 105 °C for 24 h and weighed (m_f). TSM was expressed as the percentage of sample dry matter dissolved after 24 h immersion in distilled water and determined by the following equation:

$$\text{TSM (\%)} = \frac{m_0 - m_f}{m_0} \times 100$$

2.8. Fourier transform infrared spectroscopy (FTIR)

The IR spectra for blends were obtained using a Varian 600-IR Series FTIR equipped with horizontal attenuated total reflectance (ATR) crystal (ZnSe). The spectra were collected in absorbance mode on sample powders obtained by grinding pellets in an agate mortar and placed directly onto the ATR crystal. Each spectrum is the result of the average of 32 scans at 4 cm^{-1} resolution. Measurements were recorded between 4000 and 700 cm^{-1}. All spectra were smoothed using the Savitzky–Golay function. Second-derivative spectra of the amide region were used at peak position guides for the curve fitting procedure, using OriginPro 8.6 software.

2.9. Statistical analysis

Data were subjected to one-way analysis of variant (ANOVA) by means of a SPSS computer program (SPSS Statistic 20.0). Post hoc multiple comparisons were determined by the Tukey's test with the level of significance set at $P < 0.001$.

3. Results and discussion

Extrusion is generally defined as a process used to mix, homogenize, and shape material by forcing it through a specifically designed opening. Extrusion process variables are critical factors to be considered as they impact significantly upon ingredient blends, especially those employing proteins, which ultimately impact on final film properties. Thermal extrusion exposes proteinaceous ingredients to high temperature, high pressure, and mechanical shear, which converts an ingredient like soy protein into a continuous plastic "melt", resulting in protein denaturation (Harper,

Table 1
Effect of gum arabic (ARA), carboxymethylcellulose (CMC), and dextran (DEX) content on specific mechanical energy (SME), piece density (PD), expansion ratio (ER), moisture content (MC) and total soluble matter (TSM).

	SME (kJ/kg)	PD (g/cm^3)	ER	MC (%)	TSM (%)
Control	972 ± 20.13^a	1.63 ± 0.14^a	1.12 ± 0.14^a	17.36 ± 0.05^a	31.49 ± 0.06^a
ARA3	972 ± 29.16^a	1.62 ± 0.12^a	1.13 ± 0.07^a	18.88 ± 0.07^a	31.42 ± 0.03^a
ARA6	648 ± 15.21^b	1.60 ± 0.26^a	1.14 ± 0.16^a	14.65 ± 0.26^{bc}	36.51 ± 0.56^b
ARA9	612 ± 10.91^c	1.59 ± 0.34^a	1.15 ± 0.16^a	13.79 ± 0.21^b	38.65 ± 0.23^b
CMC3	972 ± 31.51^a	1.63 ± 0.19^a	1.12 ± 0.12^a	18.36 ± 0.51^a	30.55 ± 0.21^a
CMC6	648 ± 20.11^b	1.65 ± 0.12^a	1.05 ± 0.04^b	15.49 ± 0.29^b	30.27 ± 0.09^a
CMC9	648 ± 22.31^b	1.66 ± 0.06^a	1.03 ± 0.09^b	15.13 ± 0.49^b	30.38 ± 0.61^a
DEX3	1044 ± 45.51^e	1.64 ± 0.17^a	1.10 ± 0.16^{ab}	18.70 ± 0.51^a	31.01 ± 0.07^a
DEX6	900 ± 32.53^d	1.63 ± 0.16^a	1.12 ± 0.23^a	14.53 ± 0.32^{bc}	32.35 ± 0.47^{ab}
DEX9	900 ± 35.91^d	1.61 ± 0.24^a	1.13 ± 0.32^a	12.75 ± 0.41^c	33.87 ± 0.53^b

$^{a–e}$Two means followed by the same letter in the same column are not significantly ($P > 0.001$) different through the Tukey' multiple range test.

1989). Within the process, the main fractions of SPI (7S and 11S globulins) undergo a complex pattern of association–dissociation reactions (Cheftel, Cuq, & Lorient, 1985). The effect of extrusion is to disassemble proteins and then reassemble them using disulfide bonds, hydrogen bonds, and non-covalent interactions forming fibrous extrudates. Therefore, extruded blends of various ingredients provide an excellent model system to study the effects of extrusion parameters on protein structure and to monitor protein–carbohydrate interactions, where carbohydrate ingredients have been added.

3.1. Effect of polysaccharides on extruder parameters and physical properties

Firstly, the effect of polysaccharide content on SME values was analyzed and results are shown in Table 1. The SME value indicates the extent of molecular breakdown that mechanical force undergoes during the extrusion process, so this value is an important parameter since it can influence final product characteristics (Godavarti & Karwe, 1997). Since SME is the amount of mechanical energy dissipated as heat inside the material, expressed per unit mass of the material (Harper, 1989), increasing polysaccharide content in this study resulted in higher heat transfer from the extruder barrel to the feed material and consequently, a lower viscosity, lower shear, and lower friction during extrusion. The higher the polysaccharide content (6–9%), the lower the torque and SME ($P < 0.001$) observed. Because of the reduction of the force required to push the mass through the die, a consequential reduction in friction occurred between the raw processing materials, screw shaft, and extruder barrel (Chen, Wei, & Ojokoh, 2010).

During the extrusion process, protein denaturation takes place, as has been described previously (Guerrero, Beatty, Kerry, & de la Caba, 2012), which leads to the decrease of electrostatic repulsions and allows intermolecular interactions and network formation to occur (Song, Tang, Wang, & Wang, 2011). The nature of these interactions and the structure of the network formed may affect the macroscopic properties of the blends. The reduction in conformational freedom would explain the reason for the decrease ($P < 0.001$) in moisture absorption shown in lower MC values, when polysaccharides were added (Table 1). Conversely, TSM values increased ($P < 0.001$) when the polysaccharide content in blends increased, probably due to the reduction of protein–protein interactions in the presence of polysaccharides and due to the formation of a less tight polymeric network. These facts were confirmed by FTIR analysis, as shown below.

3.2. Effect of polysaccharides on protein structure

Firstly, the band corresponding to amide I depends on the secondary structure of the protein backbone and it is the most commonly used band for the quantitative analysis of secondary structures. Secondly, the band associated with amide II is caused mainly by C—N stretching and N—H in plane bending. Therefore, alterations of these bands might clarify to what extent polysaccharide addition to ingredient blends might assist in the stabilization of added protein, since the progressive exposure of the proteins to polysaccharides may govern the structural changes that ultimately take place during the extrusion process. In order to analyze this influence, the FTIR spectra for the blends in this target IR region are shown in Fig. 1.

When polysaccharides were added, the frequencies of the bands assigned to the amide I and II regions remained constant at 1628 cm^{-1} and 1541 cm^{-1}, respectively. However, the band assigned to carboxylate in the polysaccharides at 1587 cm^{-1} for CMC, 1600 cm^{-1} for ARA, and 1643 cm^{-1} for DEX was not detectable in the blends with SPI, indicating interactions between the protein and the polysaccharides and highlights the lower capacity of the carbohydrate molecules to form intermolecular hydrogen bonds between themselves in presence of the protein (Carpenter & Crowe, 1989). Additionally, the dominant spectral change observed was the decrease in the intensity observed for the amide I and II bands, thereby indicating conformational changes occurring through interactions between protein and the polysaccharides. These changes were quantitatively measured and results are shown in Table 2.

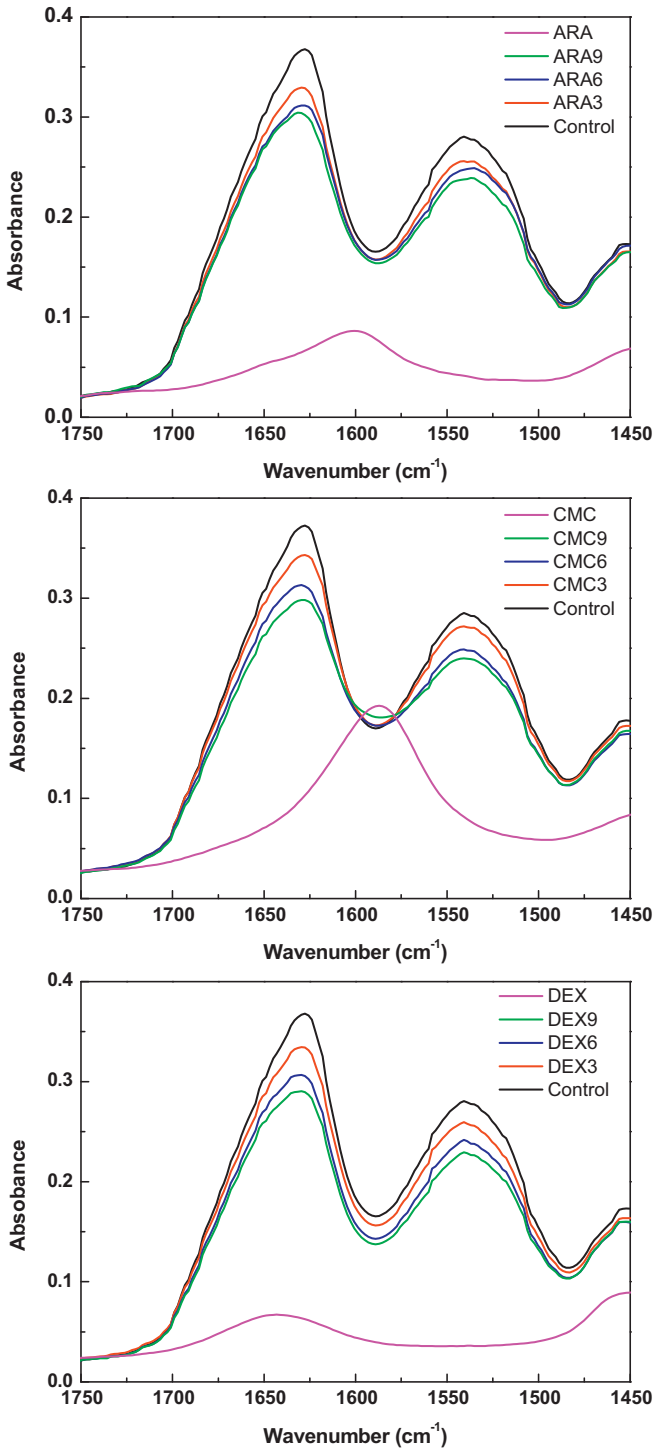

Fig. 1. Effect of polysaccharide content on FTIR spectra in the amide I and II regions for soy protein blends with gum arabic (ARA), carboxymethylcellulose (CMC), and dextran (DEX).

Table 2
FTIR absorption area values for amide I (1628 cm^{-1}), amide II (1541 cm^{-1}), and reference (2930 cm^{-1}) bands as they pertain to soy protein blends with different gum arabic (ARA), carboxymethylcellulose (CMC), and dextran (DEX) contents.

Amide area	1628 cm^{-1}	1541 cm^{-1}	2930 cm^{-1}	1628/2930 cm^{-1}	1541/2930 cm^{-1}
Control	14.624	7.649	0.168	87.048	45.530
ARA3	13.151	6.736	0.151	87.093	44.609
ARA6	12.456	5.525	0.149	83.597	37.081
ARA9	12.023	5.087	0.156	77.071	32.609
CMC3	13.666	6.896	0.157	87.045	43.924
CMC6	11.735	5.636	0.139	84.424	40.547
CMC9	10.681	4.888	0.136	78.537	35.941
DEX3	13.404	6.853	0.154	87.039	44.500
DEX6	12.579	6.143	0.152	82.757	40.414
DEX9	11.939	5.830	0.161	74.155	36.211

The relationship of amide I and II to total carbohydrate was estimated from the ratio of the absorbances at 1628 cm^{-1} and 1541 cm^{-1} to 2930 cm^{-1}. The well-defined band at 2930 cm^{-1} due to C—H content represents a good reference for total carbohydrate content, because the number of C—H groups remains constant, irrespective of changes in the ratio of polysaccharides and protein contents (Rochas, Lahaye, & Yaphe, 1986). As can be seen in Table 2, the area of the normalized bands, corresponding to amide I and II, decreased when the content of the polysaccharide increased. This change was lower for those blends containing ARA and higher for the blends containing DEX. The results indicate that carbohydrates caused changes in the infrared spectrum of soy protein, decreasing amide I and II band area and eliminating the carboxylate band, which would be indicative of the degree of hydrogen bonding occurring between proteins and carbohydrates which are necessary to provide stability to the extruded blends.

3.2.1. FTIR in amide I region

In addition to the analysis carried out above and since the band corresponding to amide I depends on the secondary structure of the protein backbone, it can also be used for the quantitative analysis of different secondary structures. Specifically, protein unfolding is characterized by changes in the intensity of the dominant band in the native protein at 1650 cm^{-1} (assigned to α-helix/unordered

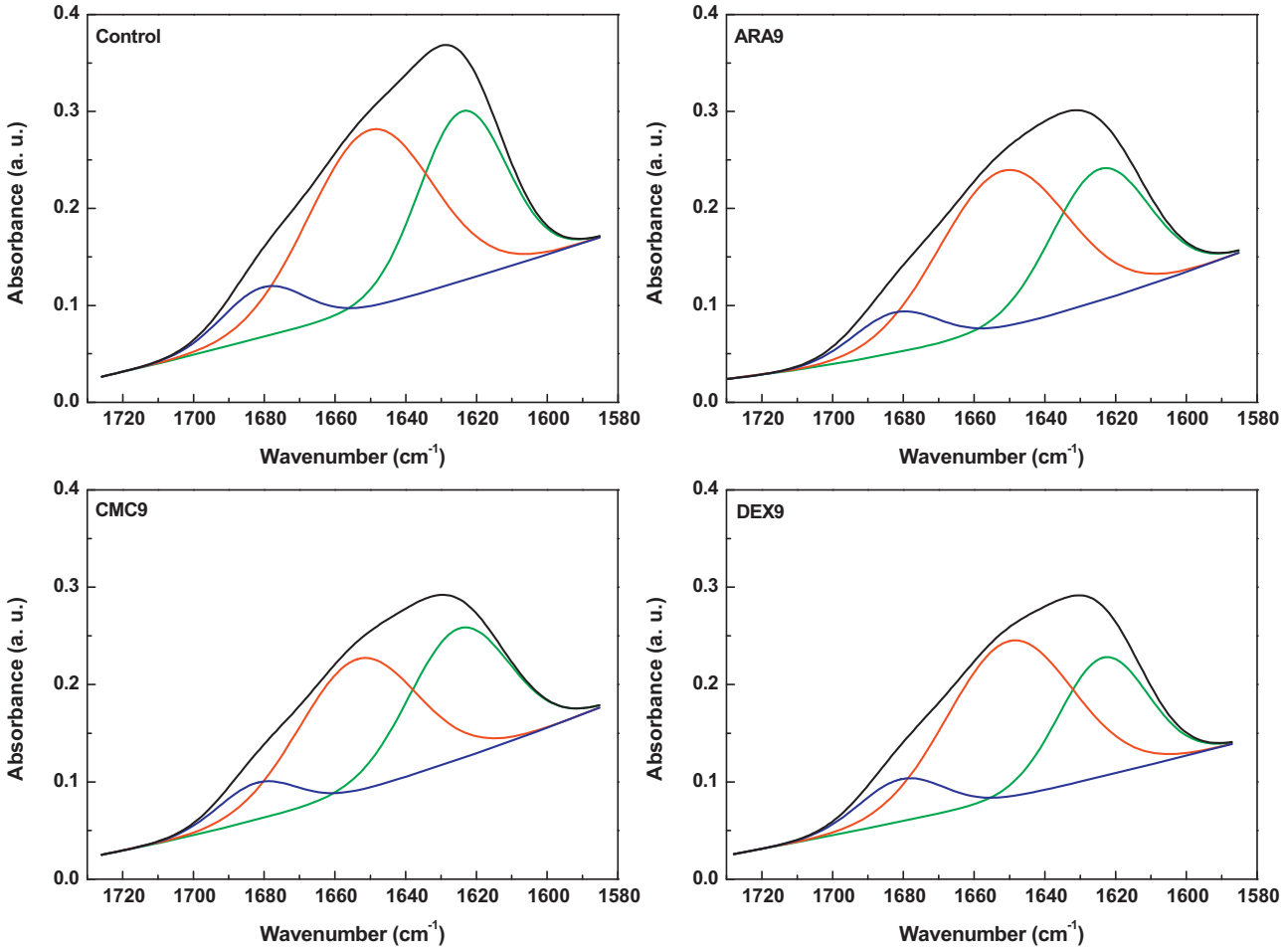

Fig. 2. Original spectrum (black) and curve fitting spectra of amide I for soy protein (control) and soy protein blends containing 9% gum arabic (ARA), carboxymethylcellulose (CMC) or dextran (DEX).

Table 3
Resulting percentage of the curve fitting of amide I for soy protein (control) and soy protein blends with different contents of gum arabic (ARA), carboxymethylcellulose (CMC) or dextran (DEX).

Area amide I	1624 cm^{-1}	1650 cm^{-1}	1680 cm^{-1}
Control	36.31	53.68	10.01
ARA3	35.77	55.02	9.21
ARA6	35.55	55.34	9.11
ARA9	35.31	55.28	9.40
CMC3	37.48	53.05	9.47
CMC6	38.67	52.10	9.23
CMC9	41.41	49.45	9.14
DEX3	35.07	54.88	10.05
DEX6	32.88	56.66	10.46
DEX9	31.14	58.59	10.27

structures) and in the regions around 1615–1630 cm^{-1} and 1680–1700 cm^{-1} (assigned to β-sheets) (Hu et al., 2010; Lefevre & Subirade, 2000), as shown in Fig. 2.

Therefore, it appears wiser to consider the individual components determined by curve fitting than a mixture of many subcomponents with slightly different frequencies. This quantitative analysis is shown in Table 3.

The area of the bands at 1624 cm^{-1}, 1650 cm^{-1}, and 1680 cm^{-1} increased, were maintained or decreased depending on the polysaccharide-type employed, thus differences in the spectra of the blends indicated that the use of different polysaccharides resulted in the production of different molecular conformations. It is worth noting that in all of the blends studied, the broad band produced at 1650 cm^{-1} reflected the presence of residual regular structures. At this position, α-helices and unordered structures are most likely to predominate in blends. Regarding the bands observed at 1624 cm^{-1} and 1680 cm^{-1}, upon increasing CMC, these two bands increased due to the formation of intermolecular antiparallel β-sheets (Lefevre, Subirade, & Pezolet, 2005). Extended antiparallel β-sheets are commonly found in aggregated proteins, especially in heat-denatured proteins (Susi, Timasheff, & Stevens, 1967). These results lead to the view that aggregation occurred and that the aggregates are partly composed of β-sheets. This observation represents a progressive conversion of residual regular structures and unordered segments into intermolecular β-sheets. The β-sheet structure has a higher degree of intermolecular hydrogen bonding and explains the important role of water molecules during the unfolding–folding process (Quinn et al., 2003). Conversely, when DEX was added to blends, the bands at 1624 cm^{-1} and 1680 cm^{-1} decreased, and the band at 1650 cm^{-1} increased, thus DEX did not represent a progressive conversion of residual regular structures and unordered segments into intermolecular β-sheets. Finally, in the case of ARA, the area of the three bands remained practically constant. The area of aggregation bands at 1680 cm^{-1} and 1624 cm^{-1} for the control indicated that 46% of the amide I band is due to intermolecular β-sheets. This behavior was maintained with the addition of ARA; however, the addition of DEX decreased intermolecular β-sheets from 46% to 41%, and intermolecular β-sheets increased from 46% to 51% when CMC was added. Therefore, it can

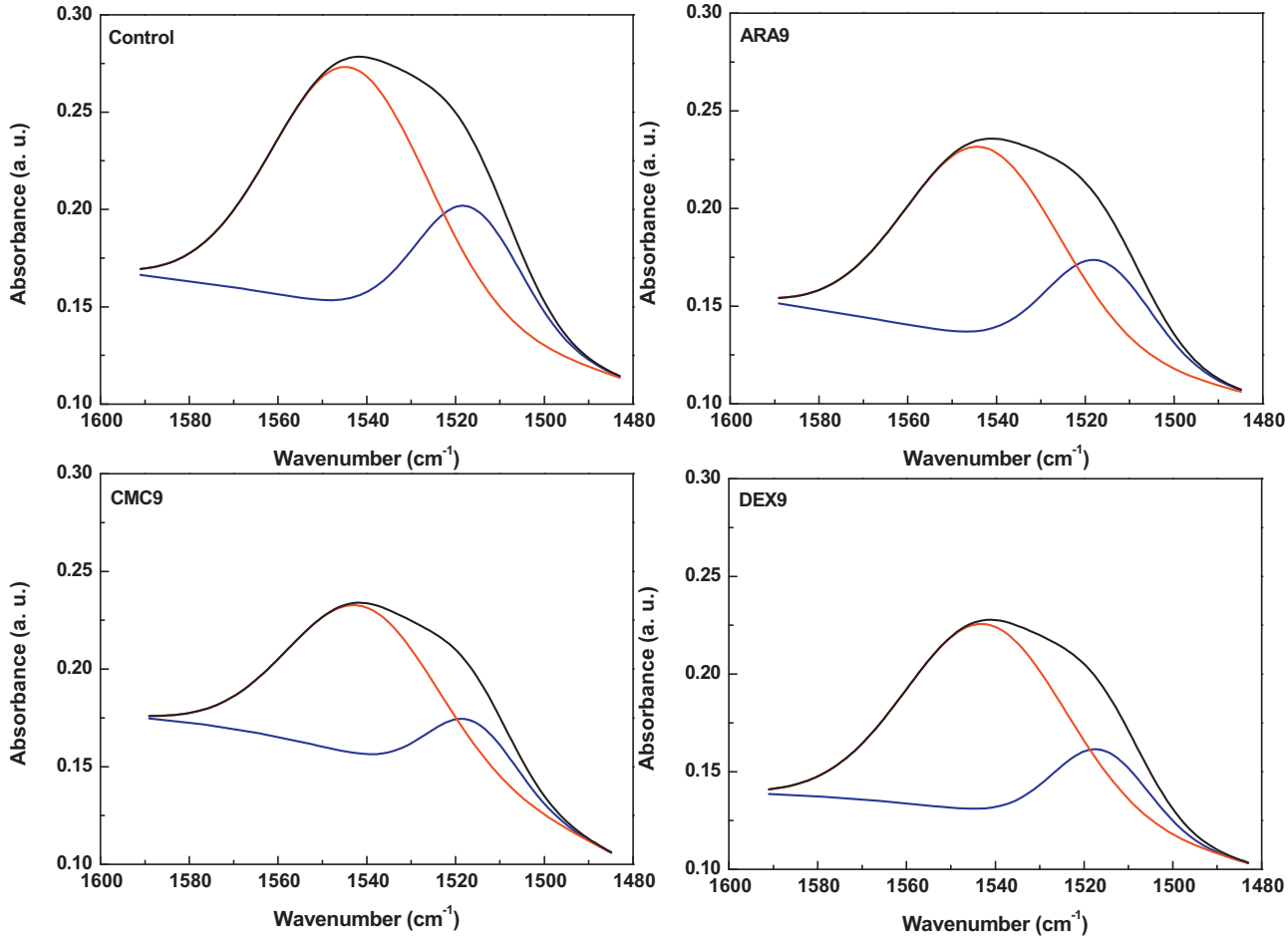

Fig. 3. Original spectrum (black) and curve fitting spectra of amide II for soy protein (control) and soy protein blends containing 9% gum arabic (ARA), carboxymethylcellulose (CMC) or dextran (DEX).

Table 4
Resulting percentage of the curve fitting of amide II for soy protein (control) and soy protein blends with different contents of gum arabic (ARA), carboxymethylcellulose (CMC) or dextran (DEX).

Area amide II	1517 cm^{-1}	1544 cm^{-1}
Control	26.49	73.51
ARA3	27.99	72.01
ARA6	27.85	72.15
ARA9	26.12	73.88
CMC3	24.72	75.28
CMC6	23.58	76.42
CMC9	22.15	77.85
DEX3	25.44	74.56
DEX6	23.78	76.22
DEX9	20.56	79.44

be estimated that between 41 and 51% of the amino acids present in blends are engaged in β-sheets, whereas 59–49% of amino acids are present in α-helix, random coil segment and turn structures. However, the polysaccharides used in this study did not lead to dramatic spectral differences in the blends. This might explain why there was no significant difference observed in some product characteristics such as density and expansion ratio (Table 1). Protein can be resistant to conformational changes during mixing and may retain its native conformation, but in the extrusion process, the protein may unfold and consequently, not regain its native conformation, resulting in conformational changes and denaturation. Regaining protein structure is dependent on the polysaccharide content and type used.

3.2.2. FTIR in amide II region

In relation to the band corresponding to amide II shown in Fig. 3, the band at 1517 cm^{-1} was attributed to the vibrational modes of tyrosine (Tyr) side chains (Hu, Kaplan, & Cebe, 2008).

The Tyr amino acids in SPI contribute at the interfaces of the β-sheet regions and act as turns, so this band provided a specific local monitor for protein conformational changes due to reduction of the conformational freedom in the protein structure (Murayama & Tomida, 2004; Reinstadler, Fabian, & Naumann, 1999), as shown quantitatively in Table 4.

4. Conclusions

Soy protein-based blends were processed by twin-screw extrusion. During trials, a decrease in extrusion torque and specific mechanic energy was achieved through the addition of polysaccharides to blends, indicating that a polysaccharide content of 6–9% in blends was enough to decrease friction and facilitate macromolecules pass through the extruder die. These improvements were the result of interactions between the extruder-induced denaturation of soy protein and polysaccharides, which was analyzed by infrared spectroscopy. The analysis of FTIR spectra in the band regions for amide I and II provided novel information about conformational changes in the protein following extrusion. Although the band frequency was maintained in a constant manner with respect to polysaccharide type and content, further analysis of each band, which can be deconvoluted into bands corresponding to the different secondary structures of the protein such as α-helix and β-sheets, showed that changes could be related to the decrease in SME values and to the changes of some physical properties like MC and TSM. This study clearly highlights the usefulness of employing FTIR as an analytical tool to assess conformational changes in the structure of proteins and interactions that have taken place between biopolymers used in blends following extrusion.

In summary, two features are the most relevant findings achieved in this work. Firstly, the utility of polysaccharide addition to facilitate the extrusion process, which is not the most widely used method to produce this type of blends nowadays, although it is the most cost effective process at industrial scale. Secondly, the value of using FTIR to analyze conformational changes in globular proteins, providing novel information to understand the relationship between protein structure and final properties of soy protein-based products.

Acknowledgments

The authors thank the University of the Basque Country (research group GIU12/06) as well as the Basque Government (projects S-PE12UN002 and S-PE13UN057) for their financial support.

References

Alves, V. D., Costa, N., & Coelhoso, I. M. (2010). Barrier properties of biodegradable composite films based on kappa-carrageenan/pectin blends and mica flakes. *Carbohydrate Polymers*, *79*, 269–276.
Andrade-Mahecha, M. M., Tapia-Blácido, D. R., & Menegalli, F. C. (2012). Development and optimization of biodegradable films based on achira flour. *Carbohydrate Polymers*, *88*, 449–458.
Archana, G., Sabina, K., Babuskin, S., Radhakrishnan, K., Fayidh, M. A., Azhagu Saravana Babu, P., et al. (2013). Preparation and characterization of mucilage polysaccharide for biomedical applications. *Carbohydrate Polymers*, *98*, 89–94.
Carpenter, J. F., & Crowe, J. H. (1989). An infrared spectroscopic study of the interactions of carbohydrates with dried proteins. *Biochemistry*, *28*, 3916–3922.
Cheftel, J. C., Cuq, J. L., & Lorient, D. (1985). In O. R. Fennema (Ed.), *Food chemistry* (pp. 245–369). New York: Marcel Dekker.
Chen, F. L., Wei, Y. M., & Ojokoh, A. O. (2010). System parameters and product properties response of soybean protein extruded at wide moisture range. *Journal of Food Engineering*, *96*, 208–213.
Doublier, J. L., Garnier, C., Renard, D., & Sanchez, C. (2000). Protein–polysaccharide interactions. *Current Opinion in Colloid & Interface Science*, *5*, 202–214.
Félix, M., Martín-Alfonso, J. E., Romero, A., & Guerrero, A. (2014). Development of albumen/soy biobased plastic materials processed by injection molding. *Journal of Food Engineering*, *125*, 7–16.
Fukushima, D., & Van Buren, J. (1970a). Effect of physical and chemical processing factors on the redispersibility of dried soy milk proteins. *Cereal Chemistry*, *47*, 571–578.
Fukushima, D., & Van Buren, J. (1970b). Mechanisms of protein insolubilization during the drying of soy milk role of disulfide and hydrophobic bonds. *Cereal Chemistry*, *47*, 687–696.
Galicia-García, T., Martínez-Bustos, F., Jiménez-Arevalo, O., Martínez, A. B., Ibarra-Gómez, R., Gaytán-Martínez, M., et al. (2011). Thermal and microstructural characterization of biodegradable films prepared by extrusion-calendering process. *Carbohydrate Polymers*, *83*, 354–361.
Gilbert, V., Rouabhia, M., Wang, H., Arnould, A. L., Remondetto, G., & Subirade, M. (2005). Characterization and evaluation of whey protein-based biofilms as substrates for in vitro cell cultures. *Biomaterials*, *26*, 7471–7480.
Godavarti, S., & Karwe, M. V. (1997). Determination of specific mechanical energy distribution on a twin-screw extruder. *Journal of Agricultural Engineering Research*, *67*, 277–287.
Gontard, N., & Guilbert, S. (1992). Edible wheat gluten films: Influence of the main process variables on film properties using response surface methodology. *Journal of Food Science*, *57*, 190–195.
Goormaghtigh, E., Cabiaux, V., & Ruysschaert, J. M. (1990). Secondary structure and dosage of soluble and membrane proteins by attenuated total reflection Fourier-transform infrared spectroscopy on hydrated films. *European Journal of Biochemistry*, *193*, 409–420.
Guerrero, P., Beatty, E., Kerry, J. P., & de la Caba, K. (2012). Extrusion of soy protein with gelatin and sugars at low moisture content. *Journal of Food Engineering*, *110*, 53–59.
Guerrero, P., Etxabide, A., Leceta, I., Peñalba, M., & de la Caba, K. (2014). Extraction of agar from *Gelidium sesquipedale* (*Rodhopyta*) and surface characterization of agar based films. *Carbohydrate Polymers*, *99*, 491–498.
Guerrero, P., Garrido, T., Leceta, I., & de la Caba, K. (2013). Films based on proteins and polysaccharides: Preparation and physical–chemical characterization. *European Polymer Journal*, *49*, 3713–3721.
Guerrero, P., Nur Hanani, Z. A., Kerry, J. P., & de la Caba, K. (2011). Characterization of soy protein-based films prepared with acids and oils by compression. *Journal of Food Engineering*, *107*, 41–49.
Harper, J. M. (1989). Food extruders and their applications. In C. Mercier, P. Linko, & J. P. Harper (Eds.), *Extrusion cooking* (pp. 1–15). Minnesota: American Association of Cereal Chemistry.
Hu, L., Hsieh, F., & Huff, H. E. (1993). Corn meal extrusion with emulsifier and soy bean fiber. *LWT-Food Science and Technology*, *26*, 544–551.

Hu, X., Kaplan, D., & Cebe, P. (2008). Dynamic protein–water relationships during β-sheet formation. *Macromolecules*, *41*, 3939–3948.
Hu, X., Lu, Q., Sun, L., Cebe, P., Wang, X., Zhang, X., et al. (2010). Biomaterials from ultrasonication-induced silk fibroin-hyaluronic acid hydrogels. *Biomacromolecules*, *11*, 3178–3188.
Klein, M., Aserin, A., Ben Ishai, P., & Garti, N. (2010). Interactions between whey protein isolate and gum arabic. *Colloids and Surfaces B: Biointerfaces*, *79*, 377–383.
Kunte, L., Gennadios, A., Cuppett, S., Hanna, M., & Weller, C. (1997). Cast films from soy protein isolates and fractions. *Cereal Chemistry*, *72*, 115–118.
Leceta, I., Etxabide, A., Cabezudo, S., de la Caba, K., & Guerrero, P. (2014). Bio-based films prepared with by-products and wastes: Environmental assessment. *Journal of Cleaner Production*, *64*, 218–227.
Lefevre, T., & Subirade, M. (2000). Molecular differences in the formation and structure of fine-stranded and particulate β-lactoglobulin gels. *Biopolymers*, *54*, 578–586.
Lefevre, T., Subirade, M., & Pezolet, M. (2005). Molecular description of the formation and structure of plasticized globular protein films. *Biomacromolecules*, *6*, 3209–3219.
Mangavel, C., Barbot, J., Popineau, Y., & Gueguen, J. (2001). Evolution of wheat gliadins conformation during film formation: A Fourier transform infrared study. *Journal of Agricultural and Food Chemistry*, *49*, 867–872.
Murayama, K., & Tomida, M. (2004). Heat-induced secondary structure and conformation change of bovine serum albumin investigated by Fourier transform infrared spectroscopy. *Biochemistry*, *43*, 11526–11532.
Quinn, G., Monahan, F. J., O'Sullivan, M., & Langares, A. (2003). Role of covalent and noncovalent interactions in the formation of films from unheated whey protein solutions following pH adjustment. *Journal of Food Science*, *68*, 2284–2288.
Reinstadler, D., Fabian, H., & Naumann, D. (1999). New structural insights into the refolding of ribonuclease T1 as seen by time-resolved Fourier-transform infrared spectroscopy. *Proteins: Structure, Function, and Bioinformatics*, *34*, 303–316.
Rochas, C., Lahaye, M., & Yaphe, W. (1986). Sulfate content of carrageenan and agar determined by infrared spectroscopy. *Botanica Marina*, *29*, 335–340.
Rodríguez, J. M., & Pilosof, A. M. R. (2011). Protein–polysaccharide interactions at fluid interfaces. *Food Hydrocolloids*, *25*, 1925–1937.
Salarbashi, D., Tajik, S., Ghasemlou, M., Shojaee-Aliabadi, S., Shahidi Noghabi, M., & Khaksar, R. (2013). Characterization of soluble soybean polysaccharide film incorporated essential oil intended for food packaging. *Carbohydrate Polymers*, *98*, 1127–1136.
Song, F., Tang, D. L., Wang, X. L., & Wang, Y. Z. (2011). Biodegradable soy protein isolate-based materials: A review. *Biomacromolecules*, *12*, 3369–3380.
Subirade, M., Kelly, I., Gueguen, J., & Pezolet, M. (1998). Molecular basis of film formation from a soybean protein: Comparison between the conformation of glycinin in aqueous solution and in films. *International Journal of Biological Macromolecules*, *23*, 241–249.
Susi, H., Timasheff, S. N., & Stevens, L. (1967). Infrared spectra and protein conformations in aqueous solutions: I. The amide I band in H_2O and D_2O solutions. *Journal of Biological Chemistry*, *242*, 5460–5466.
Wang, L., Xiao, M., Dai, S., Song, J., Ni, X., Fang, Y., et al. (2014). Interactions between carboxymethyl konjac glucomannan and soy protein isolate in blended films. *Carbohydrate Polymers*, *101*, 136–145.
Wang, C. H., & Damodaran, S. J. (1991). Thermal gelation of globular proteins. *Journal of Agricultural and Food Chemistry*, *39*, 433–438.